Developmental Biology **213,** 101–115 (1999)
Article ID dbio.1999.9320, available online at http://www.idealibrary.com on IDEAL®

Inhibition of Neural Crest Migration in *Xenopus* Using Antisense Slug RNA

Timothy F. Carl,* Christopher Dufton,† James Hanken,* and Michael W. Klymkowsky†,[1]

**Environmental, Population, and Organismic Biology and †Molecular, Cellular, and Developmental Biology, University of Colorado at Boulder, Boulder, Colorado 80309*

Based primarily on studies in the chick, it has been assumed that the zinc finger transcription factor *Slug* is required for neural crest migration. In the mouse, however, *Slug* is not expressed in the premigratory neural crest, which forms normally in *Slug* −/− animals. To study the role of *Slug* in *Xenopus laevis,* we used the injection of *XSlug* antisense RNA and tissue transplantation. Injection of *Slug* antisense RNA did not suppress the early expression of the related gene *XSnail,* but led to reduced expression of both *XSlug* and *XSnail* in later stage embryos, whereas the expression of another neural crest marker, *XTwist,* was not affected. Down-regulation of *XSlug* and *XSnail* was associated with the inhibition of neural crest cell migration and the reduction or loss of many neural crest derivatives. In particular, the formation of rostral cartilages was often highly aberrant, whereas the posterior cartilages were less frequently affected. The effects of *Slug* antisense RNA on neural crest migration and cartilage formation were rescued by the injection of either *XSlug* or *XSnail* mRNA. These studies indicate that *XSlug* is required for neural crest migration, that *XSlug* and *XSnail* may be functionally redundant, and that both genes are required to maintain each other's expression in the neural crest development of *xenopus laevis.*

Key Words: **epithelial to mesenchymal transition; neural crest; *Slug; Snail; Xenopus laevis;* cartilage.**

INTRODUCTION

The neural crest is a distinct population of embryonic cells found only in vertebrates (Gans and Northcutt, 1983; Hall and Horstädius, 1988). These ectodermally derived cells form two regional populations that emerge from the dorsolateral region of the neural tube (see Sadaghiani and Thiebaud 1987; Hall and Horstädius, 1988; Le Douarin *et al.,* 1994; Bronner-Fraser, 1995a). Cranial neural crest cells emigrate in three discrete streams—mandibular, hyoid, and branchial (shown schematically in Fig. 1)—contributing to the skull as well as the cranial ganglia and musculature (see Noden, 1983; Le Douarin *et al.,* 1993). Trunk neural crest cells emigrate and form sensory and autonomic neurons, melanocytes, enteric neurons of the gut, and endocrine cells of the adrenal gland (see Anderson, 1997; Groves and Bronner-Fraser, 1999). Given that neural crest derivatives contribute to many of the structures of the vertebrate head, modifications in the regulation of crest cells are likely to have played a prominent role in the generation of morphological diversity during vertebrate evolution (Bronner-Fraser, 1995b; Gans and Northcutt, 1983; Graveson, 1993; Mayor *et al.,* 1999).

The formation of the neural crest is regulated by a variety of signaling molecules including Wnts (Saint-Jeannet *et al.,* 1997; Chang and Hemmati-Brivanlou, 1998; Dorsky *et al.,* 1998; LaBonne and Bronner-Fraser, 1998), FGFs (Mayor *et al.,* 1997; Murphy *et al.,* 1994), noggin (Marchant *et al.,* 1998; Mayor *et al.,* 1997), and BMP-4 (Marchant *et al.,* 1998). Subsequently, neural crest migration and differentiation involves concerted changes in cell adhesion (Nakagawa and Takeichi, 1995, 1998; Duband *et al.,* 1995), matrix adhesion (Krotoski and Bronner-Fraser, 1990), cytoskeletal organization/composition (see Erickson *et al.,* 1987; Haendel *et al.,* 1996; Liu and Jessell 1998), and gene expression (see Anderson, 1997; Erickson and Reedy, 1998). The development of the neural crest exemplifies the generalized process by which embryonic cells differentiate from their original epithelial state to form mesenchyme. Such epithelial to mesenchymal transitions (EMTs) are critical to normal morphogenesis.

In vertebrates, epithelia are characterized by the expression of distinctive cytoskeletal elements (e.g., keratin-type intermediate filaments) and distinctive adhesion junctions

[1] To whom correspondence should be addressed at MCDB, UC Boulder, Boulder, CO 80309-0347. Fax: (303) 492-7744. E-mail: klym@spot.colorado.edu.

0012-1606/99 $30.00

(e.g., desmosomes and tight junctions). The EMT process consists of the coordinated remodeling of these elements. In both the chick (Nieto *et al.,* 1994) and *Xenopus laevis* (Mayor *et al.,* 1995), premigratory neural crest cells express the protein Slug (see Sefton *et al.,* 1998; Mayor *et al.,* 1999), which appears to be necessary and sufficient for inducing the disassembly of desmosomes during FGF-induced EMT in rat NBT-II bladder carcinoma cells (Savagner *et al.,* 1997).

Vertebrate *Slug* is related to the *Drosophila* gene *Snail,* which is involved in mesoderm formation (see Alberga *et al.,* 1991; Leptin, 1991). *Drosophila Snail* encodes a Zn-finger transcription factor that represses the expression of neuroectodermal genes in the mesoderm (Leptin, 1991) and is required for the invagination of mesodermal cells during gastrulation (Ip *et al.,* 1994). *Drosophila* contains a second *Snail*-like gene, named *Escargot* (Whiteley *et al.,* 1992), that has been implicated in the maintenance of diploidy in imaginal cells (see Fuse *et al.,* 1994). In tracheal cells, *Escargot* is required for normal expression of the cell adhesion molecule DE-cadherin (Tanaka *et al.,* 1996) and the control of cell fusion (see Samakovlis *et al.,* 1996). A third, more distantly related *Snail*-like gene, *Scratch,* appears to be involved in the regulation of neuronal development (Roark *et al.,* 1995). Both *Snail* and *Escargot* proteins have similar DNA binding specificity and have been proposed to act as repressors through interactions with the corepressor C-terminal binding protein (Nibu *et al.,* 1998). Whether their positive effects on target genes are direct or indirect remains to be determined. Interestingly, during *Drosophila* wing development it appears that *Snail* and *Escargot* act to maintain each other's expression through a process of auto- and cross-activation (see Fuse *et al.,* 1996).

To date only a single *Snail*-like gene, and no *Slug*-like gene, has been discovered in urochordate ascidians (Corbo *et al.,* 1997) and the cephalochordate amphioxus (Langeland *et al.,* 1998), suggesting that the vertebrate progenitor contained only a single *Snail*-like gene. In amphioxus, *Snail* is expressed in the paraxial mesoderm (Langeland *et al.,* 1998). In the zebrafish, two *Snail*-like genes (*Snail-1* and *Snail-2*) have been described (Hammerschmidt and Nusslein, 1993; Thisse *et al.,* 1993, 1995); neither contains the 29-amino-acid sequence motif characteristic of other vertebrate *Slug*s (see Sefton *et al.,* 1998). Zebrafish *Snail-1* (*ZSnail-1*) is distributed widely up to the blastula stage and, as in *Drosophila,* is associated with mesoderm formation. During gastrulation *ZSnail-1* becomes restricted to the involuting cells of the germ ring and is absent from cells of the dorsal midline. Later in development, *ZSnail-1* is found in the paraxial mesoderm, neural crest cells, and mesoderm-derived portions of the head (Thisse *et al.,* 1993; Hammerschmidt and Nusslein-Volhard, 1993). The zebrafish *Snail*-2 gene is expressed during gastrulation in cephalic mesendodermal cells and is later restricted to the neural crest (Thisse *et al.,* 1995).

In *X. laevis,* and other "higher" vertebrates, there are distinct *Snail*- as well as *Slug*-like genes. Previous studies have found that the expression of *XSnail* begins at stage 9, prior to gastrulation, in the dorsal marginal zone and progresses laterally to the ventral side of the embryo by stage 10 (Sargent and Bennett, 1990; Essex *et al.,* 1993). *XSnail* expression is subsequently found in the lateral plate mesoderm up through tailbud stage and in ectoderm, premigratory neural crest, and their derivatives, such as the branchial cartilages (Mayor *et al.,* 1993). In contrast *XSlug* is initially expressed only in prospective neural crest and is not found in early developing mesoderm (Mayor *et al.,* 1995). In the chick *CSlug,* but not *CSnail,* is expressed in the primitive streak, ingressing mesodermal cells, and premigratory neural crest (Sefton *et al.,* 1997). *CSnail* is expressed preferentially in the right side lateral mesoderm, where it appears to play an important role in the development of asymmetry (Isaac *et al.,* 1997). In the mouse, *MSnail* is expressed in the premigratory neural crest, whereas *MSlug* is not (Sefton *et al.,* 1998; Jiang *et al.,* 1998). Thus, all three of these organisms (i.e., *X. laevis,* chick, and mouse) display distinct and different patterns of expression of *Snail*/*Slug* genes during early development.

The effects of depleting or removing endogenous *Slug* have been studied directly in chick and mouse. Treatment of chick embryos with antisense oligonucleotides directed against *Slug* mRNA leads to the inhibition of *Slug* expression and neural crest migration (Nieto *et al.,* 1994). In

FIG. 1. Schematic representation of cranial neural crest migration in *Xenopus.* A stage 28 *X. laevis* embryo seen in lateral view (A). The most rostral stream of neural crest (1) gives rise to the rostral cartilages (green) such as Meckel's cartilage (M). The hyoid stream (2) contributes to the ceratohyal cartilage (CH, in red), and the branchial stream (3) contributes to the ceratobranchial or gill cartilages (CB, in yellow). A dorsal view of ventral cartilages at stage 48 (B) depicts the lower jaw, the hyobranchial skeleton, and the cartilaginous otic capsules (OC). The basihyal (Bh) and otic capsules have no contribution from the neural crest. Adapted, by permission of the publisher, from Sadaghiani and Thiebaud (1987).

FIG. 2. Effects of *XSlug* antisense RNA on the expression of *XSlug.* Embryos injected with GFP RNA at the one- or two-cell stage often express fluorescence on only one side (A—bright field; B—epifluorescence). Both A and B are pigmented embryos. All embryos displayed expressed green fluorescence on only the left side as exemplified in A and B. The inset in B displays a number of such "left-side-only" albino embryos. (C) *XSlug* RNA expression in a normal (GFP-injected-only control) stage 18 albino embryo, visualized by *in situ* hybridization. (B, D, and E) *XSlug* antisense and GFP RNA-injected stage 18 embryos display reduced expression of *XSlug* RNA on the same side as the green fluorescence. (F) Dramatic loss of *XSlug* expression is shown in a pigmented embryo, which shows a view of the developing trunk region that has almost a complete loss of endogenous *XSlug* expression on the side that had previously expressed the GFP protein. A–E are stage 18/19, F is at stage 20+; all embryos are in dorsal view with anterior at the top.

1

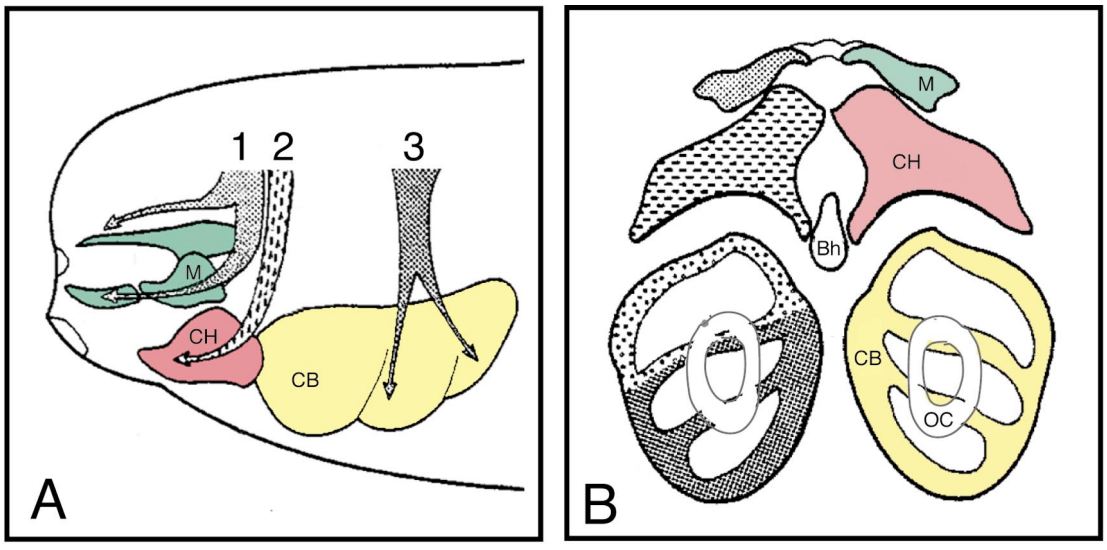

2

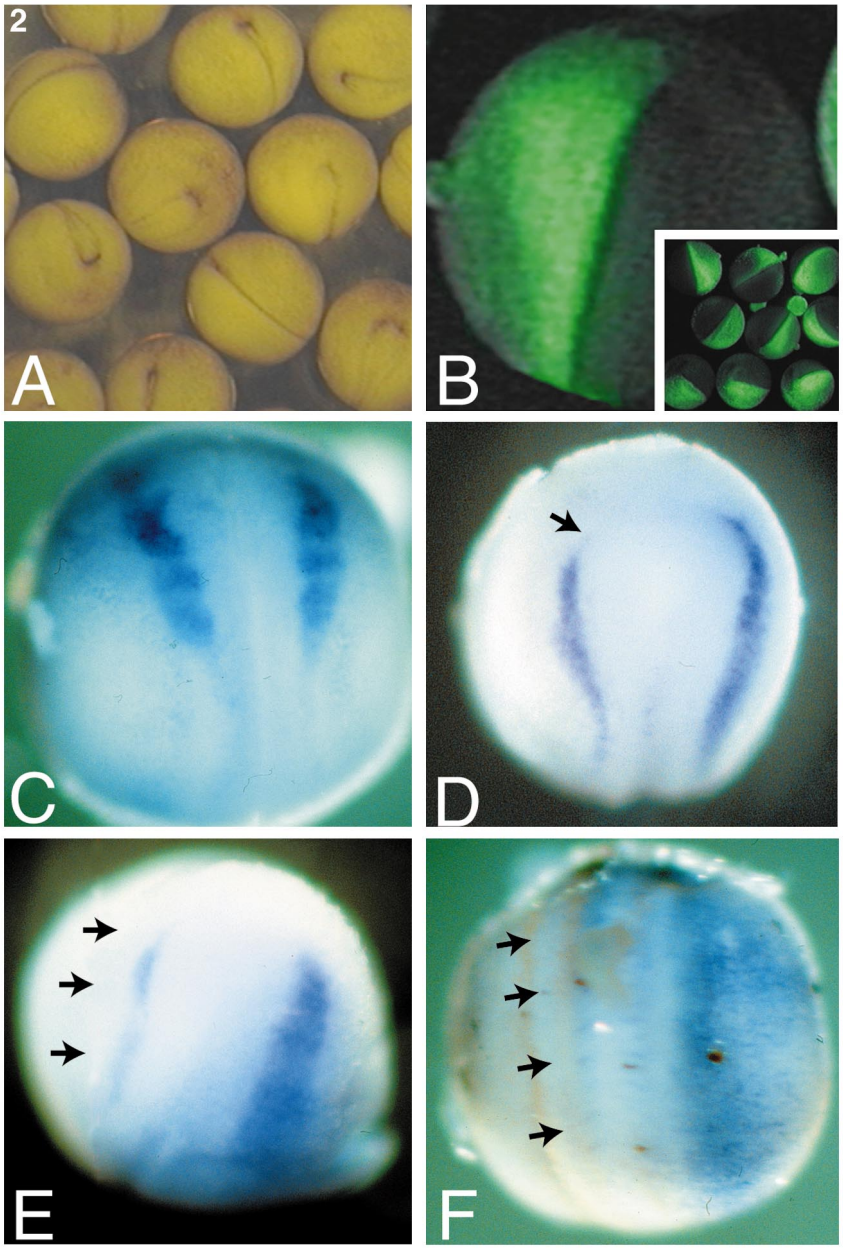

contrast, mice homozygous for a null mutation in *Slug* are viable and display no obvious defects in neural crest formation, migration, or development (Jiang *et al.*, 1998). It has been suggested that mouse may use the closely related gene *Snail* in place of *Slug* (Sefton *et al.*, 1998), although this hypothesis has not yet been tested directly.

To determine if *Slug* function is critical for neural crest differentiation/migration in *X. laevis* we have used the injection of antisense RNA targeted to the 3′ UTR of the *XSlug* mRNA to down-regulate *XSlug* expression. *XSlug* antisense RNA injection caused reduced expression of both *XSlug* and *XSnail* in post-gastrula-stage embryos, inhibited neural crest cell migration, and led to a reduction or loss of neural crest derivatives such as pigment cells and cranial cartilages. Rostral cartilages appeared more sensitive to *XSlug* antisense RNA and were often missing altogether, whereas posterior cartilages were affected less frequently. The effects of *XSlug* antisense RNA were rescued by co-injection of either *XSlug* or *XSnail* mRNAs. This study indicates that *XSlug* is required for neural crest migration, that *XSlug* and *XSnail* may be functionally redundant, and that both genes are required to maintain each other's expression in neural crest development.

MATERIALS AND METHODS

Embryo generation and tissue transplantation. Eggs were obtained from hormone-stimulated female *X. laevis* and fertilized *in vitro* following established lab procedures. Fertilized eggs were dejellied using 2% cysteine (pH 8.0) and reared at room temperature in 10% Holtfreter's solution. Larvae were staged according to the normal table of Nieuwkoop and Faber (1967). In *X. laevis*, cranial neural crest migration begins in the late neurula (stage 19). Tissue grafts were performed before migration, at stages 16 to early 19 (see Sadaghiani and Thiebaud, 1987). Embryos were placed in petri dishes lined with 2% agar and covered with 10% Holtfreter's antibiotic (gentamycin, 80 mg/L). Small segments of the cranial neural folds from host embryos were removed and replaced by comparable segments from green fluorescent protein (GFP)-labeled donors (Zernicka-Goetz *et al.*, 1996; Carl *et al.*, 1999). Care was taken to remove the overlaying ectoderm. Grafts were held in place initially with modeling clay and the embryos maintained at 16°C in Holtfreter's antibiotic. Specimens were viewed with a Power Macintosh 6500/275 and Microimage i308 video system linked to a stereo dissecting microscope equipped with epifluorescence optics.

In situ hybridization and section analysis. *XSlug* and *XSnail* cDNA-containing plasmids were generously supplied by Michael Sargent (NIMR, Mill Hill, UK). *XTwist* (Hopwood *et al.*, 1989) cDNA was generously supplied by John Gurdon (Wellcome/Cambridge). *In situ* hybridization was performed using digoxigenin–UTP-labeled antisense RNA according to standard methods (Hemmati-Brivanlou *et al.*, 1990) with minor modifications (see http://spot.colorado.edu/~klym/methods.html). The probes used for this analysis were directed against the entire coding region for *XTwist* or against the 3′ UTRs of *XSlug* and *XSnail* to ensure specificity. Typically, *in situ* analysis was done on albino *Xenopus;* when pigmented animals were used they were bleached overnight using Dent's bleach (Klymkowsky and Hanken, 1991). Paraffin sections were prepared as described in Humason (1979), with slight modification (see http://spot.colorado.edu/~klym/methods.html). Cartilage staining employed standard procedures (Klymkowsky and Hanken, 1991; Carl and Klymkowsky, 1999). Anatomical terminology follows Trueb and Hanken (1992).

Plasmid construction, RNA synthesis, and embryo injection. Polymerase chain reaction (PCR) was used to isolate the full coding region of *XSlug* and incorporate unique *Eco*RI and *Nhe*I sites at the 5′ and 3′ ends of the amplified DNA (primers used were 5′CCCGAATTCTatgccacgatctttctgg and 3′CCCGCTAGCctaatgtgctacacagcaac). The amplified DNA was then subcloned into the pCS2-mGFP (Klymkowsky, 1999) or pCS2mt (Rupp *et al.*, 1994) plasmid to create pCS2-mGFP-*XSlug* and pCS2mt-*XSlug*, respectively. The pCS2mt-GFP plasmid (Rubenstein *et al.*, 1997) was used to make mtGFP RNA. *XSnail* RNA was transcribed from the pMX51*cDNA*XSna*SP72 plasmid. To generate capped mRNA, we used a SP6 mMessage mMachine kit (Ambion). The pCS2 plasmids were linearized with *Sac*II. To generate *XSlug* antisense RNA, the pMX363**XSlug**sp72 plasmid, which contains only the 3′ UTR of the *XSlug* cDNA, was linearized with *Eco*RV and transcribed using an Ambion MegaScript kit. An NIH BLAST Search using the sequence of the *XSlug* 3′ UTR failed to identify any regions of sequence similarity with the *XSnail* UTR or any other *X. laevis* cDNAs (data not shown).

RNA (total volume 20 nl) was injected into either the animal pole region of fertilized eggs or one of two blastomeres at the two-cell stage, following standard procedures (see Rubenstein *et al.*, 1997). Embryos were reared under standard laboratory conditions. Uninjected embryos and embryos injected with GFP RNA (5 ng) alone were used as controls for the injection procedure. In a typical *XSlug* antisense RNA experiment 2.6 ng of the antisense RNA was co-injected with the GFP RNA. In "rescue" experiments fertilized eggs were injected with 2.6 ng of *XSlug* antisense RNA, together with 5 ng GFP RNA and various concentrations of *XSlug* or *XSnail* RNAs. A standard χ^2 test was used to calculate the *P* values for these experiments.

RT-PCR analysis. RNA was extracted from groups of five embryos. Three hundred nanograms of total RNA from stage 6, 9, and 13 embryos was reverse transcribed with MuLV reverse transcriptase primed with random hexamers (Perkin–Elmer GeneAmp PCR). cDNA was subject to 40 cycles of PCR at an annealing/extension temperature of 57°C using upstream (5′-CAATGCAAGAACTGTTCC-3′) and downstream (5′-TCTAGGCAAGAATTGCTC-3′) primers to amplify a 367-bp fragment of *XSlug* or upstream (5′-AAGCACAATGGACTCCTT-3′) and downstream (5′-CCAATAGTGATACACACC-3′) primers to amplify a 294-bp region of *XSnail* (LaBonne and Bronner-Fraser, 1998)

RESULTS

To determine if *Slug* expression is required for neural crest migration in the frog *X. laevis*, we tested the effectiveness of *XSlug* antisense RNA in down-regulating endogenous *XSlug* expression. One- and two-cell embryos were injected with uncapped *XSlug* antisense RNA, together with capped RNA encoding a six-myc-tagged $S_{65}\rightarrow T$ mutated form of the GFP as a cell lineage marker. Neurula (stage 15) embryos were sorted based on the pattern of green fluorescence. Embryos displaying fluorescence (Figs. 2A and 2B) were fixed at stage 18–22 and examined by *in situ* hybridization. Of these specimens, one-third displayed reduced levels of both *XSlug* (Figs. 2D–2F) and *XSnail* (Figs.

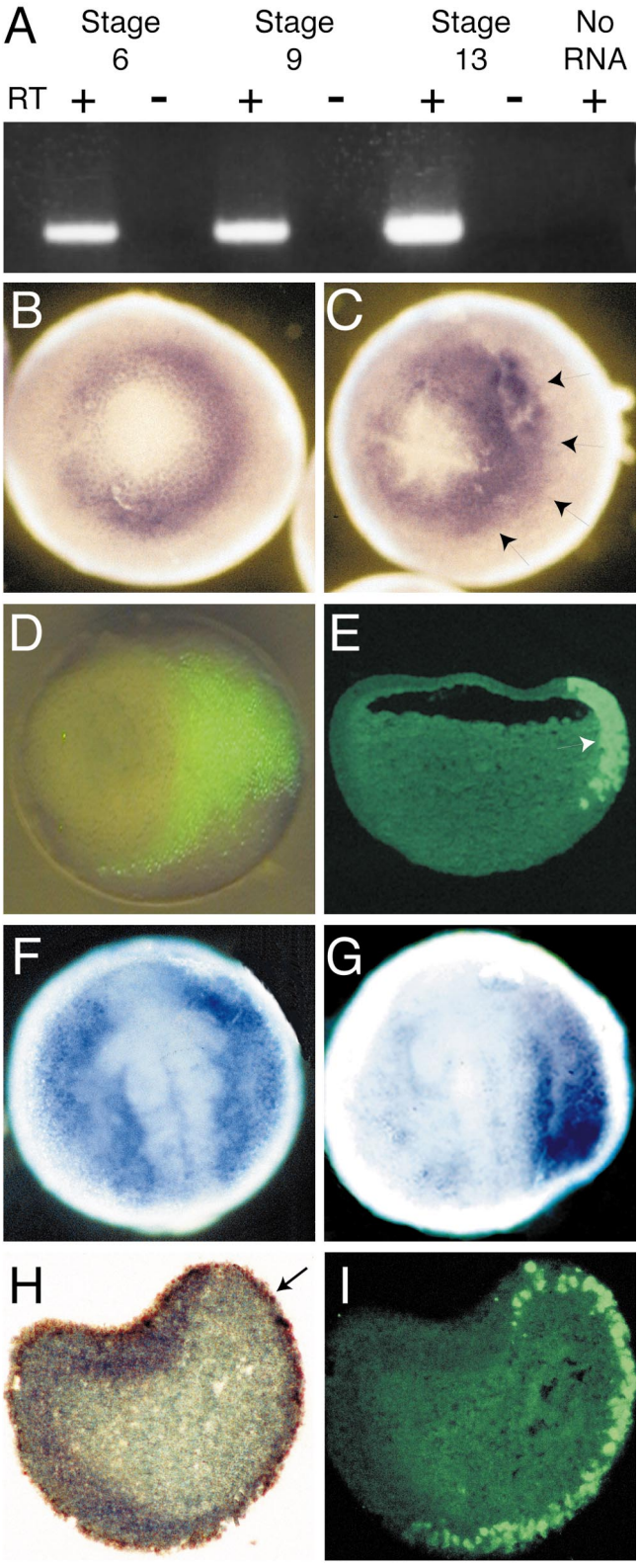

FIG. 3. *XSlug* antisense RNA effect on the expression of *XSnail*. (A) RT-PCR analysis indicates that *XSlug* is present in pre-MBT stage embryos. "+" indicates the presence of reverse transcriptase in the RT-PCR reaction, "−" indicates no reverse transcriptase controls. At stage 10/10+, a ring of involuting mesodermal cells express *XSnail* (B). Embryos were injected with *XSlug* antisense RNA at the two-cell stage. In stage 10–12 embryos that have been injected with *XSlug* antisense RNA (C), the expression of *XSnail* is not reduced, but often enhanced (arrows) on the side on which fluorescence had been observed earlier (D). A cross section of a stage 10+ embryo reveals that the GFP marker is found in both the ectoderm and the mesoderm (arrowhead) in the region of enhanced *XSnail* expression (E). At stage 20, *XSnail* is expressed on both sides of the embryo, but absent from the neuroectoderm (F). Injection of *XSlug* antisense RNA leads to a reduction of *XSnail* RNA on the injected side (G), and *in situ* hybridization reveals a reduction of *XSnail* RNA throughout ectodermal and mesodermal tissues in a cross section of the caudal region of a treated pigmented embryo at stage 18 (H, bright field; I, epifluorescence). Arrow in H points to ectodermal pigment. All whole mounts are shown in dorsal views with anterior at the top.

3B–3I) expression. Reduction of *XSlug*/*XSnail* expression ranged from moderate, with scattered patches of normal expression (Figs. 2D and 2E) to the complete loss of expression (Figs. 2F and 3G). A greater number of embryos exhibiting reduced levels of either gene were found when embryos were sorted for high intensity of fluorescence on either their right or their left side. Expression of another crest marker, *XTwist* (Hopwood *et al.*, 1989; Stoetzel *et al.*, 1998), was normal in midneurula embryos (Fig. 4).

As assessed by RNase protection and *in situ* hybridization, expression of *XSlug* first appears in premigratory crest (Mayor *et al.*, 1995). We therefore expected that injection of *XSlug* antisense RNA would have no effect on the early expression of *XSnail* (stage 10+) in involuting mesoderm cells. *In situ* hybridization of *XSlug* antisense RNA-injected embryos did not reduce *XSnail* expression at stage 10–12, but rather caused an apparent increase in its expression domain (Figs. 3B–3E) in approximately one-third of the specimens. Using RT-PCR we found that *XSlug* RNA was detectable in unfertilized eggs (data not shown) and in blastula-stage embryos (Fig. 3A) and is therefore a maternal transcript.

Inhibition of neural crest migration by XSlug antisense RNA. To determine whether down-regulation of *XSlug* and *XSnail* expression by *XSlug* antisense RNA disrupted neural crest migration we transplanted premigratory cranial neural crest from donor embryos injected with *XSlug* antisense and GFP RNAs, or GFP RNA alone as a control, into uninjected hosts. Donor embryos were selected at stage 15 (early neurula) based on the intensity of fluorescence in the developing cranial region. The neural fold, containing premigratory neural crest (stage 17–early 19, 19–20 h postfertilization), was removed from the host and replaced by fluorescent donor tissue. The green-fluorescent transplanted tissue could be followed in living embryos well past premetamorphic stage 50 (day 15 postfertilization).

By stage 24 (late neurula/≈26 h postfertilization) it was readily apparent whether the tissue graft was success-

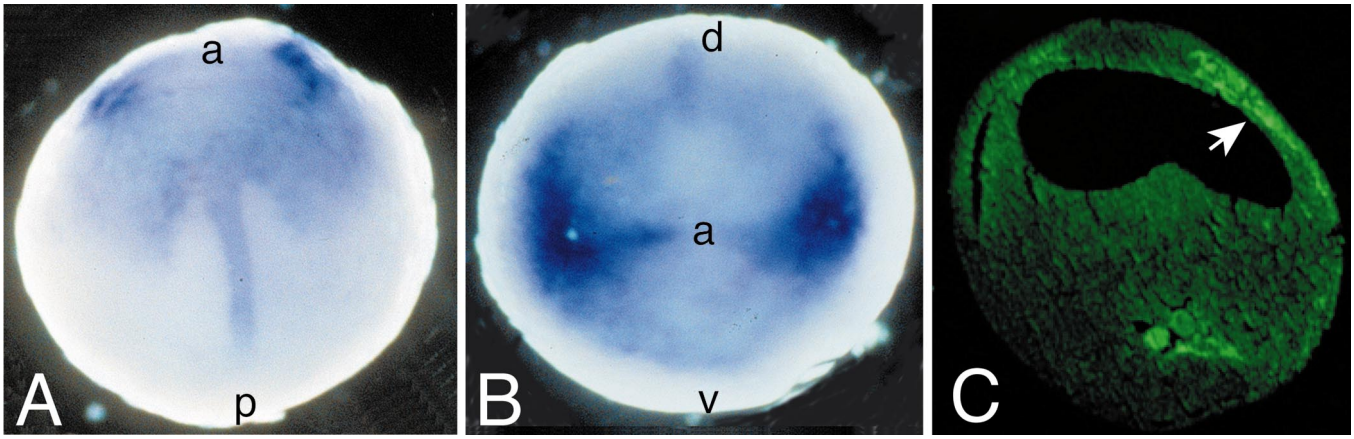

FIG. 4. *XTwist* expression. Embryos were injected with *XSlug* antisense and GFP RNAs, selected for fluorescence on the left side (as in Fig. 2), and analyzed for *XTwist* expression using *in situ* hybridization at stage 16–18. No change was observed between uninjected control embryos (data not shown) and embryos injected with *XSlug* antisense and GFP RNA (A—dorsal view with anterior "a" to the top and posterior "p" at the bottom. B—anterior view with anterior "a," posterior "p," dorsal "d," and ventral "v" axes marked). (C) A section of such an embryo stained for the myc-epitope present on the GFP protein. It shows that the GFP marker is present in dorsal mesodermal (arrowhead) and ectoderm.

ful and if donor neural crest cells had begun migration. Sixty-two percent of the GFP control embryos showed normal migration of the cranial neural crest streams (Figs. 5A and 5B). In contrast, when *XSlug* antisense RNA was co-injected with GFP RNA, only 15% of the transplanted neural crest streams migrated normally (Figs. 5C and 5D). To determine the specificity of the *XSlug* antisense RNA-induced migration defect, embryos were injected with *XSlug* antisense RNA, GFP RNA, and RNA encoding either myc- or mycGFP-tagged forms of *XSlug* or an untagged form of *XSnail* RNA. Both forms of *XSlug* which do not contain the *XSlug* 3′ UTR were made in the pCS2mt plasmid. Both *XSlug* and *XSnail* sense RNAs efficiently rescued the *XSlug* antisense RNA migration defect (Fig. 5E). Reduction of the amount of co-injected *XSlug* RNA reduced the frequency and extent of rescue.

As a second assay for migration, we examined the neural crest marker *XTwist* in late-stage specimens that had been injected with antisense *XSlug* RNA. Embryos that expressed the GFP marker on only the left side (Fig. 6A) were used for this experiment. *In situ* hybridization was performed on each specimen at stages 24–28, which were then sectioned and stained for GFP. The expression of *XTwist* was affected on the side of the embryo containing the GFP marker in most of the specimens observed. The affects ranged from moderate (Figs. 6, 1L, and 6, 2L) to severe (Fig. 6, 3L). On the side that did not express the GFP marker highly, there was little or no reduction in *XTwist* expression (Figs. 6, 1R–6, 3R). The most severe loss of migration, revealed by *XTwist* expression, was often noticed in specimens in which the GFP was found in both the ectoderm and the mesoderm (Fig. 6, 3s).

FIG. 5. *XSlug* antisense RNA hinders neural crest migration, assessed by transplantation. When cranial crest is transplanted from the GFP RNA-injected donor into an uninjected host, migration occurs normally in most embryos (A—bright field of transplanted embryo and B—epifluorescence view). In contrast, crest migration is often blocked when the donor tissue is taken from embryos injected with *XSlug* antisense/GFP RNAs (C, D). "e" marks the eye for A and B. To determine the specificity of the *XSlug* antisense RNA effect, we examined whether coexpression of epitope-tagged forms of *XSlug* rescued the neural crest migration defect induced by *XSlug* antisense RNA (E). As a control, donor specimens injected with 5 ng GFP RNA alone were transplanted into hosts. Sixty-two percent of the embryos had normal migration pattern, assessed by observing streams of neural crest labeled by GFP fluorescence. Injection of *XSlug* antisense RNA ("slug ASR") together with GFP RNA dramatically reduced the number of transplants displaying normal migration, $P = 0.0002$. Co-injection of RNAs encoding either mycGFP-*XSlug* (mG*XSlug*) or myc-tagged *XSlug* (mt*XSlug*) led to a rescue of this migration defect. Similarly, injection of *XSnail* RNA also rescued the *XSlug* antisense RNA effect. The concentrations of RNAs injected are shown along the bottom of the graph; the numbers of normally migrating transplants and the total number of transplanted embryos examined for each condition are depicted above the corresponding bar. The *P* values are $P = 0.0002$ for GFP/antisense RNA, $P = 0.016$ for GFP/antisense RNA + 0.35 ng mG*Xslug*, $P = 0.55$ for GFP/antisense RNA + 1.0 ng mG*Xslug*, $P = 0.55$ for GFP/antisense RNA + 2.1 ng mG*Xslug*, $P = 0.2$ for GFP/antisense RNA + 1.5 ng mG*Xslug*, $P = 0.35$ for GFP/antisense RNA + 1.6 ng *XSnail*.

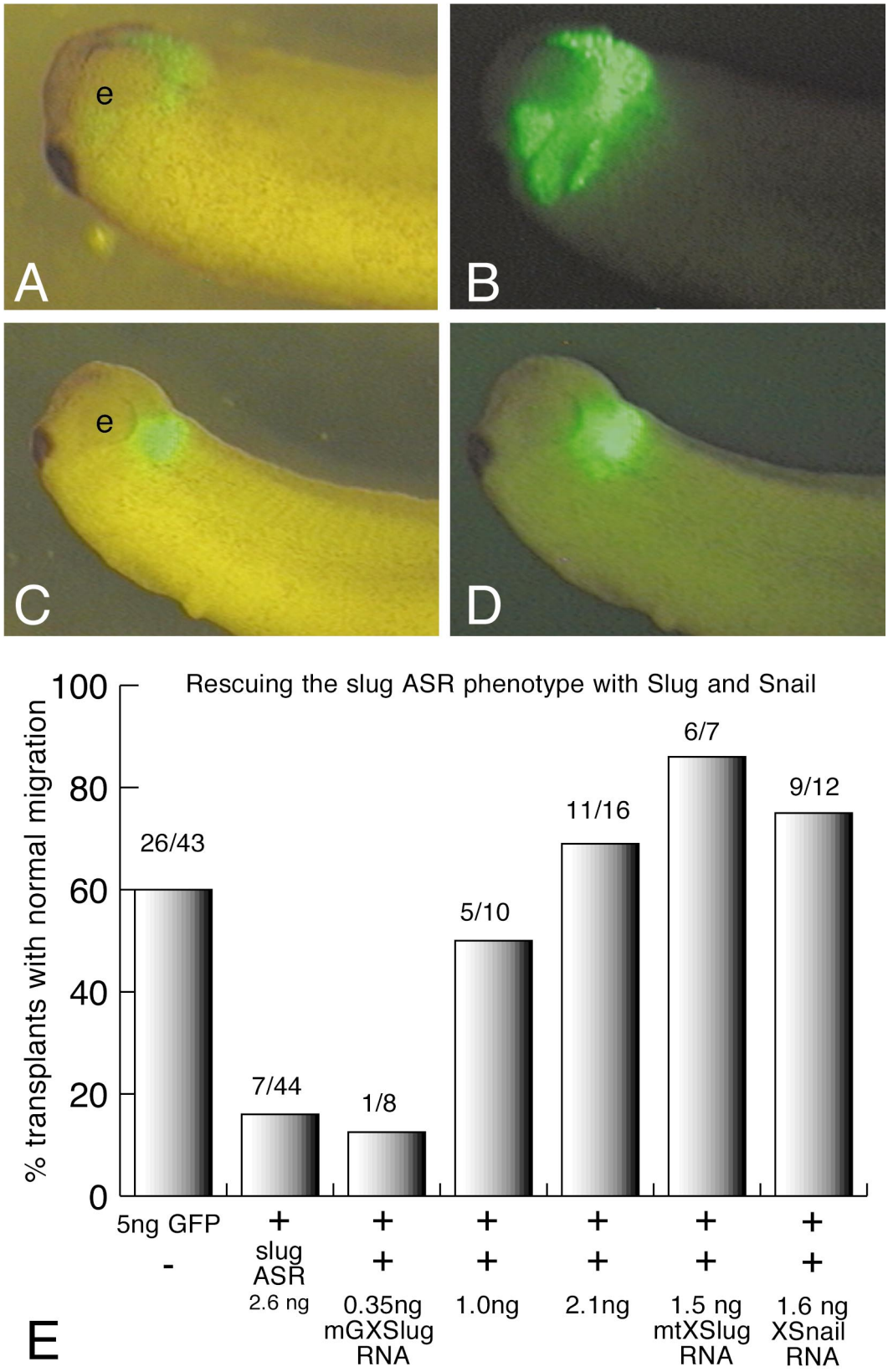

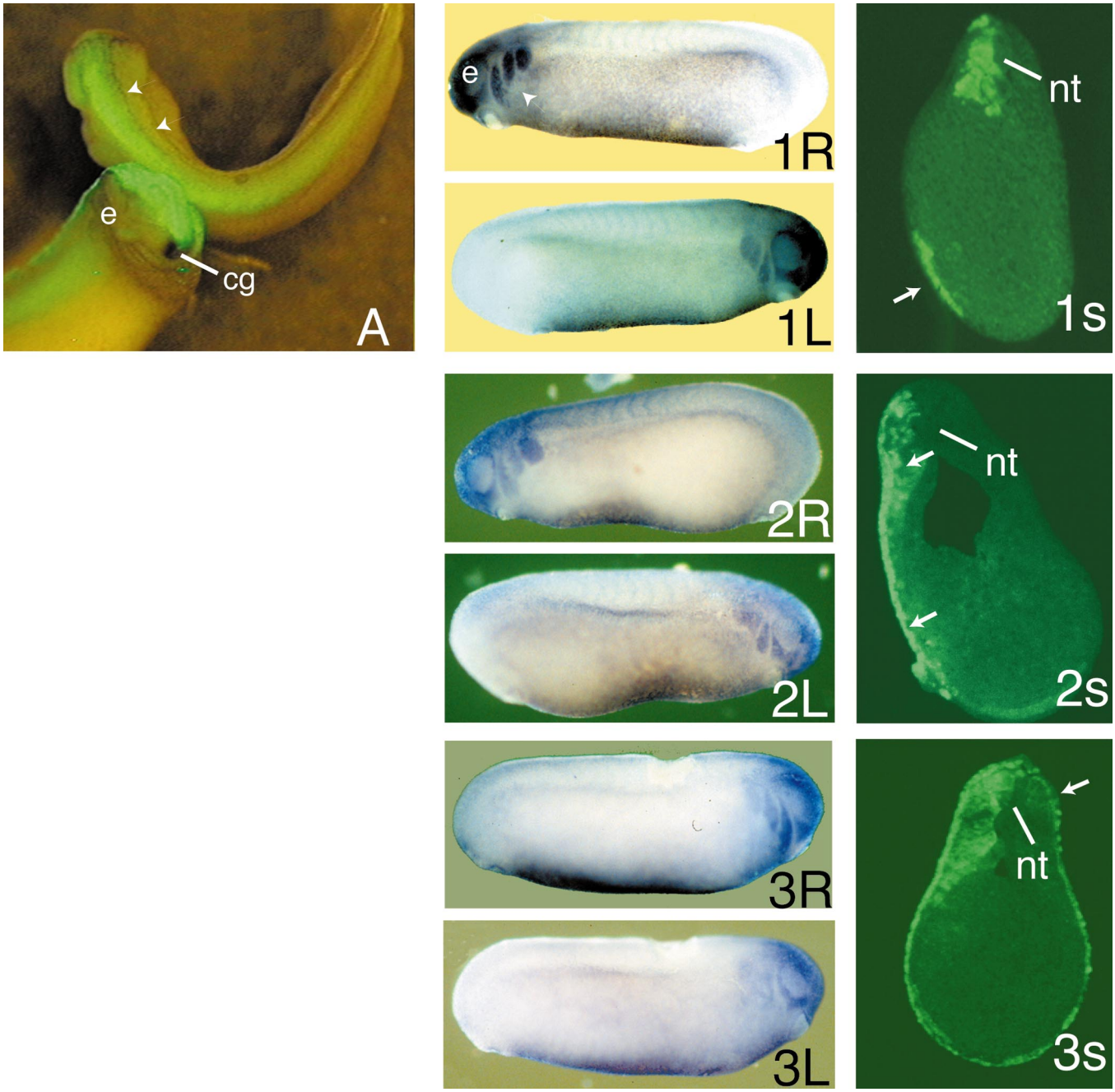

FIG. 6. *XSlug* antisense RNA hinders neural crest migration assessed by *XTwist in situ* hybridization. Specimens were injected with *XSlug* antisense and GFP RNAs at the one-cell stage, allowed to develop until neural crest migration was well under way (stage 24+), and then selected based on their expression of the GFP marker on the left side only (A, arrows; "e" marks the eye and "cg" the cement gland). Specimens were analyzed for crest migration defects by *in situ* hybridization of *XTwist*. Specimen 1 displayed GFP primarily in the dorsal mesoderm on the left-hand side (1s—"nt" marks the neural tube in 1s–3s) and in a patch of ventral ectoderm (arrow). Migration of the crest was normal on the right side (1R, arrowhead) and moderately hindered on the left (1L). Specimen 2 displayed a moderate loss of migration on the left side (2L); GFP was localized to both mesoderm (upper arrow) and ectoderm (lower arrow) on the left side (2s). Specimen 3 displayed an almost complete loss of crest migration in both the posterior streams of crest (3L) and a moderate loss of migration on the right side of the embryo (3R); GFP was found in both the mesoderm and the ectoderm on the left side and in the ectoderm on the right side (arrow) of the embryo.

TABLE 1
Cranial Cartilage Defects of Stage 47/48 Larvae Injected with *XSlug* Antisense and GFP RNAs

Cartilage morphology	Type I	Type II
Normal	14	11
Moderate	22	11
Severe	6	4
Total	42	26

Note. Type I embryos display the GFP marker on both left and right sides, whereas Type II embryos display the GFP on *only* the right or the left side. Specimens with moderate defects include those that have reduced or missing rostral cranial cartilages, and severe specimens have all cranial cartilages affected or missing.

Cranial cartilage development is affected in an antero-posterior gradient. To study the affect of *XSlug* antisense RNA on cranial cartilage development, injected embryos were separated into two group types at stage 15. Type I embryos expressed green fluorescence on both left and right sides. Type II embryos expressed green fluorescence that was limited to either their left or their right sides. The number of injected specimens that survived until stage 48–50 was relatively low ($N = 68$) (Table 1).

The larval skull at stage 47/48 is exclusively cartilaginous; cranial bone is not visible in cleared and stained whole mounts until stage 54. Posteriorly, a pair of parachordal cartilages lie on either side of, and unite for a short distance rostral to, the notochord. A cartilaginous auditory (otic) capsule is dorsal and lateral to each parachordal. Anterior parachordal cartilages extend rostrally into the paired cranial trabecula; together, these two pairs of cartilages enclose the prominent basicranial fenestra medial to the eyes. Extending laterally from the union of the anterior parachordal and cranial trabecula is the ventrolateral process of the posterior palatoquadrate. Anterior to the basicranial fenestra is a broad, medial sheet of cartilage, the ethmoidal or trabecular plate, which is fused to anterior palatoquadrate cartilages on either side. Each anterior palatoquadrate bears a posteriorly directed subocular bar, which encloses the subocular fenestra. The suprarostral plate extends rostrally from the trabecular plate to form the skeleton of the upper jaw. Lateral wings, or alae, of the suprarostral plate thin distally and begin to unite with a rostral process of the anterior palatoquadrate to form the long tentacular cartilage, which is distinctive of pipid larvae (Trueb and Hanken, 1992). Ventral to the suprarostral plate is the lower jaw, which comprises paired, Meckel's cartilages on either side of a single, median infrarostral cartilage (Figs. 7A–7C). Posterior to the lower jaw and suspended beneath the skull proper is the prominent hyobranchial skeleton. It comprises paired ceratohyal cartilages, representing the second (hyoid) visceral arch—a small, median copula (basibranchial cartilage), which partly overlaps the ceratohyals posteriorly, and a series of four ceratobranchial cartilages (arches 3–6). Ceratobranchial cartilages on either side are united medially, by a broad hypobranchial plate, as well as laterally. Together with the copula they form a single branchial, or gill, basket on each side of the head.

At stage 47/48 (5.5–7.5 days postfertilization), cranial morphology in control embryos (injected with GFP RNA only) was virtually identical to that in uninjected embryos, except for a slight increase in the asymmetry of paired cartilages, especially posteriorly (Figs. 7A and 7B). *XSlug* antisense RNA injection, however, significantly altered skeletal patterning. The magnitude of effects varied widely among the cleared and stained Type I embryos, which defined a continuum from little or no change (i.e., normal morphology), to moderate defects, to extreme defects (Table 1). The severity of defects displayed a pronounced craniocaudal gradient: moderate defects were confined to rostral cartilages (Figs. 7D–7F), whereas defects involving posterior cartilages were found only in specimens with the most severe cranial dysmorphology (Fig. 7G–7I). Type II embryos displayed the same craniocaudal gradient, but lacked neural crest-derived cartilage on the injected side only (Table 1, Figs. 7J–7L). Morphology of the non-neural-crest-derived basihyal and otic capsular cartilages was not affected, even in the most severe cases, indicating that the affects of *XSlug* antisense RNA on cranial development are restricted to neural crest-derived cartilages.

XSlug antisense RNA injection causes reduced melanocyte formation. To assess the effects of *XSlug* antisense RNA on cells derived from trunk neural crest, we examined melanophore number and distribution in larvae between stages 28 and 48. The number and distribution of melanocytes observed in uninjected larvae were not discernibly altered in embryos injected with GFP RNA only (Figs. 8A, 8C, and 8D). Injection of *XSlug* anti-sense RNA, however, altered the distribution and apparent size of melanocytes (FIG. 8B, E and F). In the mildest cases there was only a slight decrease in the numbers of melanocytes (data not shown). Specimens that displayed severe effects had noticeably fewer melanocytes that appeared reduced in size (Fig. 8B). In some specimens the effect appeared mosaic, with the complete loss of melanocytes in patches surrounded by areas displaying normal numbers of melanocytes (Figs. 8E and 8F).

DISCUSSION

Antisense RNA has a long history as an effective method to down-regulate gene expression in *X. laevis* (see Harland and Weintraub, 1985; Melton, 1985; Lallier *et al.*, 1996; Kil *et al.*, 1996; Lombardo and Slack, 1997 as examples), although the exact mechanism of its action remains poorly understood (see Nellen and Sczakiel, 1996). In our studies, we used an antisense RNA directed against the 3′ UTR of the *XSlug* cDNA isolated by Mayor *et al.* (1995) to down-regulate the expression of the endogenous *XSlug* (Fig. 2). Surprisingly, we also observed a down-regulation of the related gene *XSnail* (Fig. 3). The specificity of *XSlug* antisense RNA was demonstrated by the ability of RNAs

containing the *XSlug* coding region to rescue the negative antisense effect in a dose-dependent manner (Fig. 5E) and the fact that the expression of other neural crest markers, such as *XTwist* (Fig. 4), was not affected prior to crest migration.

Antisense XSlug RNA caused a decrease in neural crest migration. To determine whether *XSlug* antisense RNA disrupted neural crest migration, we transplanted premigratory cranial neural crest from donor embryos injected with *XSlug* antisense and GFP RNAs into uninjected hosts (Fig. 5). Fifteen percent of the antisense-treated transplants displayed normal migration, significantly different from that found in GFP-only transplants. In addition, either *XSlug* or *XSnail* sense RNA, but not the unrelated GFP RNA, rescued the negative migration phenotype (Fig. 5E). Since the injected *XSlug* mRNAs did not contain sequences complementary to *XSlug* antisense RNA, their ability to rescue presumably reflects the ability of exogenous *XSlug* protein to rescue defects arising from the reduction or absence of endogenous *XSlug* protein. It is interesting to note that transplants containing *XSlug* RNA displayed normal migration at a slightly increased frequency than did the GFP RNA-injected controls, suggesting that *Slug* overexpression may in fact stimulate neural crest migration. LaBonne and Bronner-Fraser (1998) found that overexpression of *XSlug* caused an increase in the numbers of melanocytes, a phenotype which can be explained by an increase in the number of migrating crest cells.

The effect of *XSlug* antisense RNA on neural crest migration could also be seen in the loss of *XTwist* expression at stages at which neural crest migration was well under way (stage 24+); antisense *XSlug* RNA induced a moderate (Figs. 6, 1L, and 6, 2L) to a severe (Fig. 6, 3L) decrease in *XTwist* expression, similar to its effect on neural crest migration (Fig. 5), cartilage development (Fig. 7), and melanocyte formation (Fig. 8). Whether this loss of *XTwist* expression reflects apoptosis of aberrantly migrating neural crest cells, or some other process, is currently under study.

The range of effects of *XSlug* antisense RNA is likely the result in part of variations in its distribution within the embryo. Whereas some specimens display the GFP marker, and presumably the *XSlug* antisense RNA, in both ectoderm and mesoderm, others display the GFP marker in only a subset of tissues (Fig. 6). Specimens in which the GFP marker was present in both the ectoderm and the mesoderm typically displayed the most severe effects. When the GFP marker was observed in only the ectoderm there was often a reduction of *XSnail* in the mesodermal tissues as well (Fig. 3), suggesting that the antisense RNA diffuses beyond the boundaries of the GFP marker.

Cranial neural crest streams appear to differ in their sensitivity to XSlug levels. Whereas anterior cartilages are typically modified or even lost in *XSlug* antisense RNA-injected embryos, posterior cartilages are affected much less frequently (Fig. 7). These rostrocaudal differences correspond with differences in the particular migratory stream that gives rise to the various cartilages (Fig. 1; Sadaghiani and Thiebaud, 1987). Mandibular and hyoid streams generate most cartilages of the rostral half of the skull (e.g., Meckel's, ceratohyal), whereas virtually all caudal crest-derived cranial cartilages are derived from the branchial streams. Cranial cartilages that are not derived from cranial neural crest, e.g., basihyal, otic capsules (Stone, 1926; Olsson and Hanken, 1996), were not affected by *XSlug* antisense RNA injection.

It is unlikely that the rostrocaudal gradient in the effects of *XSlug* antisense RNA on cranial morphology is due to localized differences in levels of *XSlug* antisense RNA. For example, one may imagine that the antisense RNA was more highly localized in the most rostral regions in animals that displayed the loss of rostral structures. But green fluorescence, derived from the co-injected GFP RNA, was regularly present in caudal regions of treated embryos,

FIG. 7. Cranial skeletal defects in *XSlug* antisense RNA-injected larvae. Dorsal (A) and ventral (B) views of a normal *X. laevis* tadpole (stage 47) stained with Alcian blue reveal cranial cartilages (C—schematic drawing of ventral cranial cartilages and otic capsules, depicted as in Fig. 1B). Type I (green fluorescence *not* restricted to either the left or the right side of the embryo) *XSlug* antisense RNA-injected embryos often displayed moderate (D–F) to severe (G–I) defects in neural crest-derived cartilages. Typically, anterior cartilages were reduced or missing in treated specimens. As a result, the remaining anterior neurocranium (trabecular plate) was either long and thin, usually tapering at the rostrum, or foreshortened and bluntly pointed. The lower jaw was either extremely reduced or absent on both sides (in D it comprises a single cartilage), and the ceratohyal becomes a single, triangular or V-shaped cartilage (D, E, red arrows). Separate articulating Meckel's and infrarostral cartilages are not present as such (black arrow; F—schematic representation of the phenotype). Most anterior cartilages are missing in the most severely affected animals (G, H). In G the jaw is missing and the cereatohyal is reduced (black arrow). In H the anterior half of the skull is ablated. (I—schematic representation of this phenotype). In all Type I *XSlug* antisense RNA-injected larvae, non-neural crest-derived skeletal elements, i.e., otic capsules and the basihyal cartilage, and the crest-derived ceratobranchial cartilages were unaffected. In Type II embryos (green fluorescence restricted to either the left or the right side of the embryo; J, K), neural crest-derived cranial cartilage morphology was normal on the nonfluorescent (left) side, but highly abnormal on the fluorescent/*XSlug* antisense RNA (right) side. Defects include absence of Meckel's cartilage (black arrows) from the lower jaw and reduction (J) or absence (K—red arrow) of the ceratohyal cartilages. The most severely affected Type II specimens displayed a complete loss of all cranial cartilages, with the exception of non-neural crest cartilages (e.g., basihyal and otic capsules) on the injected side (L—schematic representation of the severest phenotype). Bh, basihyal; CB, ceratobranchial; CH, ceratohyal; G, gut; IR, infrarostral cartilage; M, Meckel's cartilage; OC, otic capsule; PC, parachordal cartilage; SR, suprarostral plate; T, trabecula; TP, trabecular plate.

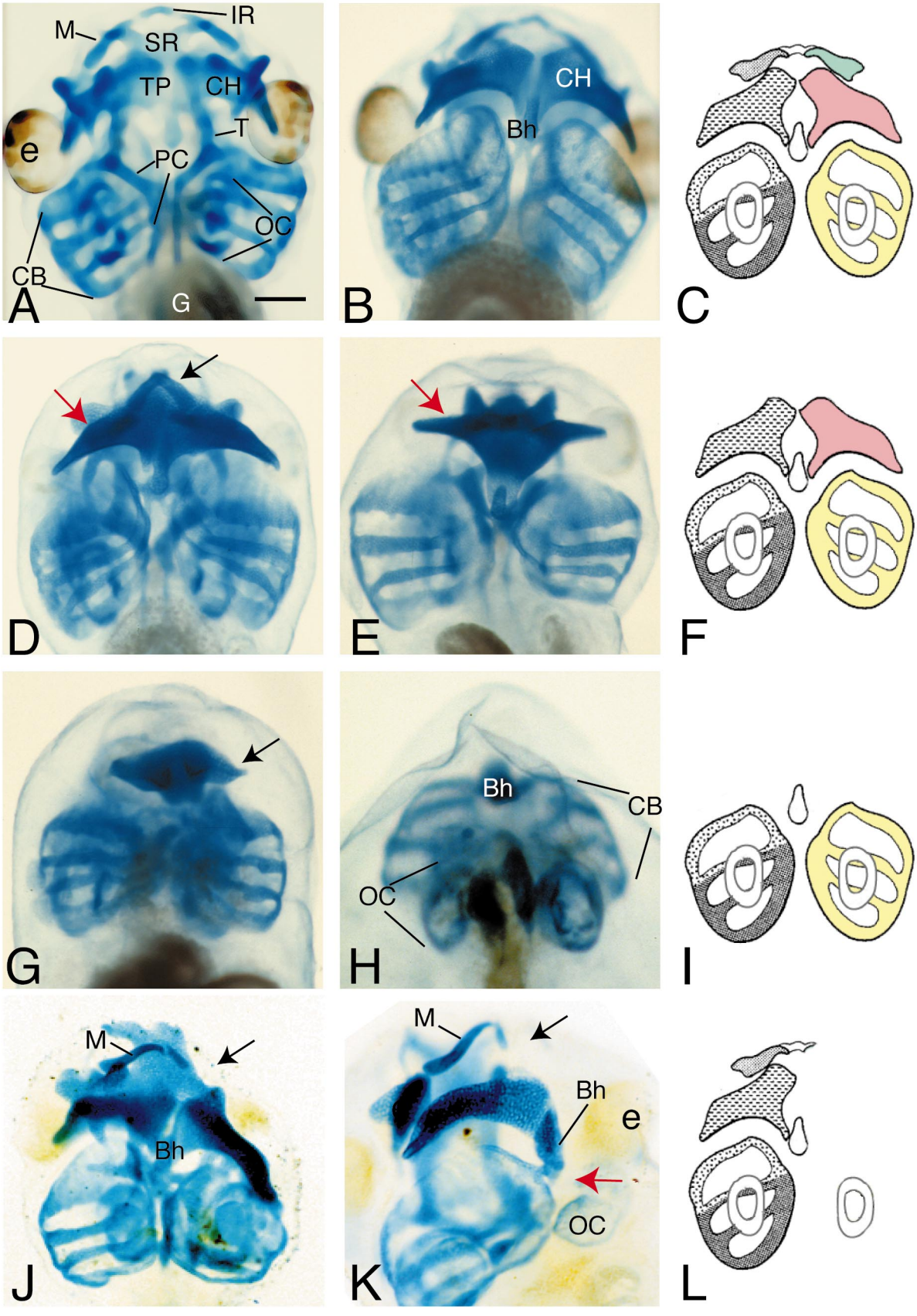

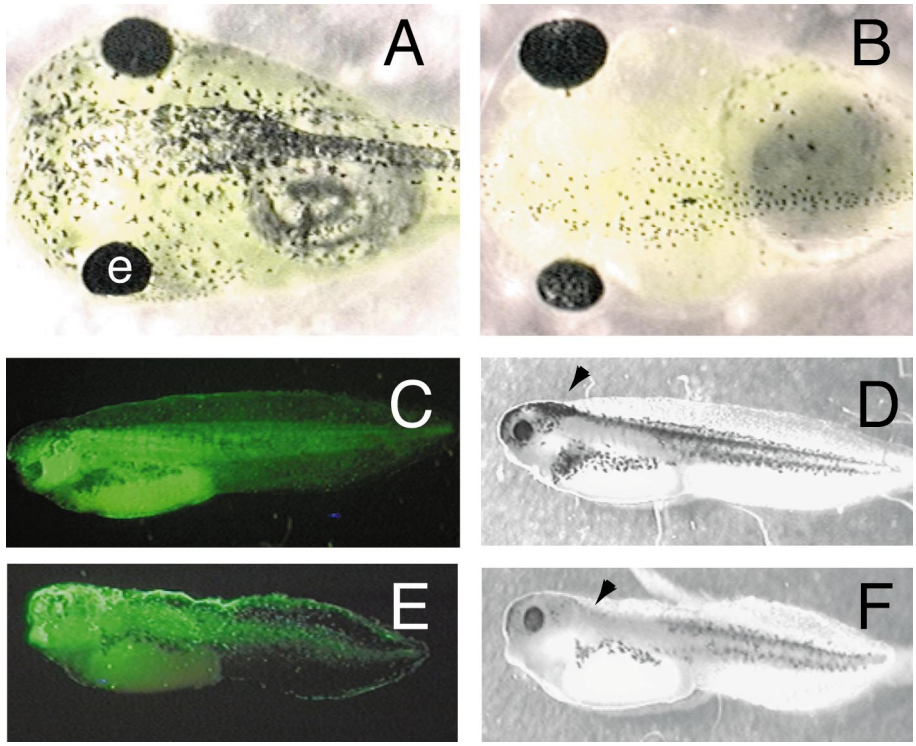

FIG. 8. Affect of *XSlug* antisense RNA on melanocytes. (A, B) Stage 48 larvae in dorsal view. (A) Normal pigmentation of a control larvae injected with GFP RNA only. (B) Normal pigmentation is often dramatically reduced in both number and apparent size of melanocytes of larvae injected with *XSlug* antisense RNA. (C, D) Control GFP RNA only injected larvae display a normal pattern of melanocyte distribution (arrowhead in D points to the dorsomedial stripe located in the head). In a *XSlug* antisense RNA/GFP RNA-injected larvae (E, F), loss of melanocytes ranges from moderate (F) to severe (see B). Arrowhead in F points out the absence of the dorsomedial stripe. Larvae in C–F are at stage 40/41.

including those exhibiting the most severe rostral defects. Moreover, we often observed reduction of melanocyte numbers in individuals that displayed only slight defects in the anterior cranial cartilages, suggesting that the antisense RNA was distributed throughout the specimen. Also, no specimen was found in which caudal cranial cartilages were modified while rostral cartilages were not. These results indicate that particular streams of cranial crest have different sensitivities to *XSlug* levels. This difference in sensitivity may be due to the fact that while rostral cranial cartilages are derived primarily from the neural crest, the more caudal cranial cartilages are formed by both neural crest and surrounding mesenchymal cells (Sadaghiani and Thiebaud, 1987).

Cross-regulation of Snail by Slug. Perhaps the most surprising result to emerge from our studies was the down-regulation of *XSnail* expression in embryos injected with *XSlug* antisense RNA (Fig. 3). Nieto *et al.* (1994) used antisense oligonucleotides directed against the *CSlug* coding region to examine its role in neural crest development. While treatment of chick embryos with these antisense oligonucleotides clearly induced a transient decrease in *CSlug* expression, and an inhibition of neural crest migration, no data on the effect on *CSnail* expression was presented (although antisense oligos directed against *CSnail* did not affect neural crest differentiation).

It has previously been reported that in *Xenopus,* the expression of *XSnail* begins at stage 9, prior to gastrulation, in the dorsal marginal zone and progresses laterally to the ventral side by stage 10 (Sargent and Bennett, 1990; Essex *et al.*, 1993). In contrast, *XSlug* expression is not detected until stage 11, at which it is found in an arc on the dorsal side of the embryo (Mayor *et al.*, 1995). Using RT-PCR we show that both *XSlug* (Fig. 3A) and *XSnail* (data not shown) are maternally expressed. At stage 10, embryos injected with *XSlug* antisense RNA showed no decrease in the level of *XSnail,* but rather displayed an apparent increase in the level of *XSnail* expression (Figs. 3B–3E). This was in distinct contrast to later stages, at which *XSnail* RNA levels were down-regulated, similar to that seen in *XSlug* (Fig. 3F–3I). This raises the possibility that in *X. laevis* expression of *XSlug* has two roles with respect to *XSnail.* In the formation of early mesoderm *XSlug* appears to be involved in negatively regulating the expression of *XSnail,* whereas in neural crest *XSlug* may have a positive effect on *XSnail* expression.

The apparent dependence of *XSnail* expression on *XSlug* expression, as well as the ability of both *XSlug* and *XSnail* to rescue the neural crest migration defect induced by *XSlug* antisense RNA (Fig. 5E), leads us to conclude that in *X. laevis* neural crest *Slug* and *Snail* proteins play functionally similar roles. The cross-regulation of *XSlug* and *XSnail* bears a resemblance to the interaction between *Snail* and *Escargot* in the *Drosophila* wing disc (Fuse *et al.*, 1996). In that study, both *Snail* and *Escargot* functions were required for expression of *Snail* and a single functional copy of either gene was sufficient to support normal wing development. It therefore seems plausible that in *X. laevis,* and perhaps in the chick, in which expression of *CSlug* precedes expression of *CSnail* in the crest, neural crest-specific expression of *CSnail* may be dependent upon *CSlug.* Under these conditions, depletion of *Slug* appears to lead to defects in neural crest due to the absence of both *Slug* and *Snail.*

A different situation clearly applies in the mouse. The pattern of *MSnail* and *MSlug* expression is significantly different from that seen in the chick and *X. laevis* (Sefton *et al.*, 1998; Jiang *et al.*, 1998). It has been argued that the patterns of *Slug* and *Snail* expression have been "swapped" between the chick and the mouse. This in itself argues for the functional redundancy of the *Slug* and *Snail* proteins. Whether subtle differences between the two are involved in differences in neural crest-dependent morphogenic events remains to be determined.

ACKNOWLEDGMENTS

We thank M. Sargent for XSlug and XSnail cDNAs, Andy Ryscavage for constructing pCS2mt-XSlug, and John Gurdon for the XTwist clone. We also thank Linda Barlow for advice on tissue transplantation, Scott Carl for statistical assistance, Sally Susnowitz for help with an earlier version of the manuscript, and two anonymous reviewers for extremely helpful comments and suggestions. This work was supported by grants from the National Institutes of Health (GM54001 to M.W.K.), the National Science Foundation (IBN 94-19407 and 98-01586 to J.H.), and Sigma Xi, Society for Integrative and Comparative Biology, and the University of Colorado at Boulder (to T.F.C).

REFERENCES

Alberga, A., Boulay, J. L., Kempe, E., Dennefeld, C., and Haenlin, M. (1991). The *Snail* gene required for mesoderm formation in *Drosophila* is expressed dynamically in derivatives of all three germ layers. *Development* **111,** 983–992.

Anderson, D. J. (1997). Cellular and molecular biology of neural crest cell lineage determination. *Trends Genet.* **13,** 276–280.

Bronner-Fraser, M. (1995a). Origin of the avian neural crest. *Stem Cells* **13,** 640–646.

Bronner-Fraser, M. (1995b). Origins and developmental potential of the neural crest. *Exp. Cell. Res.* **218,** 405–417.

Carl, T. F., Dufton, C., Vourgourakis, Y., Klymkowsky, M., and Hanken, J. (1999). Green fluorescent protein used to assess cranial neural crest derivatives in the frog, *Xenopus laevis. In* "Regulatory Processes in Development: The Legacy of Sven Horstädius" (C. Jacobson, L. Olsson, and T. Laurent, Eds.). Portland Press, Seattle, in press.

Carl, T. F., and Klymkowsky, M. W. (1999). Visualizing endogenous and exogenous proteins in *Xenopus* (and other organisms). *In* "A Comparative Methods Approach to the Study of Oocytes and Embryos" (J. Richter, Ed.), pp. 291–315. Oxford Press, New York.

Chang, C., and Hemmati-Brivanlou, A. (1998). Neural crest induction by Xwnt7B in *Xenopus. Dev. Biol.* **194,** 129–134.

Corbo, J. C., Erives, A., Di, G. A., Chang, A., and Levine, M. (1997). Dorsoventral patterning of the vertebrate neural tube is conserved in a protochordate. *Development* **124,** 2335–2344.

Dorsky, R. I., Moon, R. T., and Raible, D. W. (1998). Control of neural crest cell fate by the Wnt signalling pathway. *Nature* **396,** 370–373.

Duband, J. L., Monier, F., Delannet, M., and Newgreen, D. (1995). Epithelium–mesenchyme transition during neural crest development. *Acta Anat.* **154,** 63–78.

Erickson, C. A., Tucker, R. P., and Edwards, B. F. (1987). Changes in the distribution of intermediate-filament types in Japanese quail embryos during morphogenesis. *Differentiation* **34,** 88–97.

Erickson, C. A., and Reedy, M. V. (1998). Neural crest development: The interplay between morphogenesis and cell differentiation. *Curr. Top. Dev. Biol.* **40,** 177–209.

Essex, L. J., Mayor, R., and Sargent, M. G. (1993). Expression of *Xenopus Snail* in mesoderm and prospective neural fold ectoderm. *Dev. Dyn.* **198,** 108–122.

Fuse, N., Hirose, S., and Hayashi, S. (1996). Determination of wing cell fate by the *Escargot* and *Snail* genes in *Drosophila. Development* **122,** 1059–1067.

Gans, C., and Northcutt, G. R. (1983). Neural crest and the origin of vertebrates: A new head. *Science* **220,** 268–274.

Graveson, A. C. (1993). Neural crest: Contributions to the development of the vertebrate head. *Am. Zool.* **33,** 424–433.

Groves, A. K., and Bronner-Fraser, M. (1999). Neural crest diversification. *Curr. Top. Dev. Biol.* **43:** 221–258.

Haendel, M. A., Bollinger, K. E., and Baas, P. W. (1996). Cytoskeletal changes during neurogenesis in cultures of avian neural crest cells. *J. Neurocytol.* **25,** 289–301.

Hall, B. K., and Horstädius, S. (1988). "The Neural Crest." Oxford Univ. Press, Oxford.

Hammerschmidt, M., and Nusslein-Volhard, V. C. (1993). The expression of a zebrafish gene homologous to *Drosophila Snail* suggests a conserved function in invertebrate and vertebrate gastrulation. *Development* **119,** 1107–1118.

Harland, R., and Weintraub, H. (1985). Translation of mRNA injected into *Xenopus* oocytes is specifically inhibited by antisense RNA. *J. Cell Biol.* **101,** 1094–1099.

Hemmati-Brivanlou, A., Frank, D., Bolce, M. E., Brown, B. D., Sive, H. L., and Harland, R. M. (1990). Localization of specific mRNAs in *Xenopus* embryos by whole-mount *in situ* hybridization. *Development* **110,** 325–330.

Hopwood, N. D., Pluck, A., and Gurdon, J. B. (1989). A *Xenopus* mRNA related to *Drosophila* twist is expressed in response to induction in the mesoderm and the neural crest. *Cell* **59,** 893–903.

Humason, G. (1979). "Animal Tissue Techniques." Freeman, San Francisco.

Ip, Y. T., Maggert, K., and Levine, M. (1994). Uncoupling gastrulation and mesoderm differentiation in the *Drosophila* embryo. *EMBO J.* **13,** 5826–5834.

Isaac, A., Sargent, M. G., and Cooke, J. (1997). Control of vertebrate left–right asymmetry by a *Snail*-related zinc finger gene. *Science* **275,** 1301–1304.

Jiang, R., Lan, Y., Norton, C. R., Sundberg, J. P., and Gridley, T. (1998). The *Slug* gene is not essential for mesoderm or neural crest development in mice. *Dev. Biol.* **198,** 277–285.

Kil, S. H., Lallier, T., and Bronner-Fraser, M. (1996). Inhibition of cranial neural crest adhesion *in vitro* and migration *in vivo* using integrin antisense oligonucleotides. *Dev. Biol.* **179,** 91–101.

Klymkowsky, M. W. (1999). Plakophilin, armadillo repeats and nuclear localization. *Microsc. Res. Tech.* **44,** 43–54.

Klymkowsky, M. W., and Hanken, J. (1991). Whole-mount staining of *Xenopus* and other vertebrates. *Methods Cell Biol.* **36,** 419–441.

Krotoski, D., and Bronner-Fraser, M. (1990). Distribution of integrins and their ligands in the trunk of *Xenopus laevis* during neural crest cell migration. *J. Exp. Zool.* **253,** 139–150.

LaBonne, C., and Bronner-Fraser, M. (1998). Neural crest induction in *Xenopus:* Evidence for a two-signal model. *Development* **125,** 2403–2414.

Lallier, T. E., Whittaker, C. A., and DeSimone, D. W. (1996). Integrin and α6-expression is required for early nervous system development in *Xenopus laevis. Development* **122,** 2539–2554.

Langeland, J. A., Tomsa, J. M., Jackman, W. J., and Kimmel, C. B. (1998). An amphioxus *Snail* gene: Expression in paraxial mesoderm and neural plate suggests a conserved role in patterning the chordate embryo. *Dev. Genes Evol.* **208,** 569–577.

LeDouarin, N. M., Ziller, C., and Couly, G. F. (1993). Patterning of neural crest derivatives in the avian embryo: *In vivo* and *in vitro* studies. *Dev. Biol.* **159,** 24–49.

LeDouarin, N. M., Dupin, E., and Ziller, C. (1994). Genetic and epigenetic control in neural crest development. *Curr. Opin. Genet. Dev.* **4,** 685–695.

Leptin, M. (1991). Twist and Snail as positive and negative regulators during *Drosophila* mesoderm development. *Genes Dev.* **5,** 1568–1576.

Liu, J. P., and Jessell, T. M. (1998). A role for rhoB in the delamination of neural crest cells from the dorsal neural tube. *Development* **125,** 5055–5067.

Lombardo, A., and Slack, J. M. (1997). Inhibition of eFGF expression in *Xenopus* embryos by antisense mRNA. *Dev. Dyn.* **208,** 162–169.

Marchant, L., Linker, C., Ruiz, P., Guerrero, N., and Mayor, R. (1998). The inductive properties of mesoderm suggest that the neural crest cells are specified by a BMP gradient. *Dev. Biol.* **198,** 319–329.

Mayor, R., Essex, L. J., Bennett, M. F., and Sargent, M. G. (1993). Distinct elements of the *xsna* promoter are required for mesodermal and ectodermal expression. *Development* **119,** 661–671.

Mayor, R., Guerrero, N., and Martinez, C. (1997). Role of FGF and noggin in neural crest induction. *Dev. Biol.* **189,** 1–12.

Mayor, R., Morgan, R., and Sargent, M. G. (1995). Induction of the prospective neural crest of *Xenopus. Development* **121,** 767–777.

Mayor, R., Young, R., and Vargas, A. (1999). Development of neural crest in *Xenopus. Curr. Top. Dev. Biol.* **43,** 85–113.

Melton, D. A. (1985). Injected anti-sense RNAs specifically block messenger RNA translation in vivo. *Proc. Natl. Acad. Sci. USA* **82,** 144–148.

Murphy, M., Reid, K., Ford, M., Furness, J. B., and Bartlett, P. F. (1994). FGF2 regulates proliferation of neural crest cells, with subsequent neuronal differentiation regulated by LIF or related factors. *Development* **120,** 3519–3528.

Nakagawa, S., and Takeichi, M. (1995). Neural crest cell–cell adhesion controlled by sequential and subpopulation-specific expression of novel cadherins. *Development* **121,** 1321–1332.

Nakagawa, S., and Takeichi, M. (1998). Neural crest emigration from the neural tube depends on regulated cadherin expression. *Development* **125,** 2963–2971.

Nellen, W., and Sczakiel, G. (1996). In vitro and in vivo action of antisense RNA. *Mol. Biotechnol.* **6,** 7–15.

Nibu, Y., Zhang, H., Bajor, E., Barolo, S., Small, S., and Levine, M. (1998). dCtBP mediates transcriptional repression by *Knirps, Kruppel* and *Snail* in the *Drosophila* embryo. *EMBO J.* **17,** 7009–7020.

Nieto, M. A., Sargent, M. G., Wilkinson, D. G., and Cooke, J. (1994). Control of cell behavior during vertebrate development by *Slug,* a zinc finger gene. *Science* **264,** 835–839.

Nieuwkoop, P. D., and Faber, J. (1967). "Normal Table of *Xenopus* Development." North-Holland, Amsterdam.

Noden, D. M. (1983). The embryonic origins of avian cephalic and cervical muscles and associated connective tissues. *Am. J. Anat.* **168,** 257–276.

Olsson, L., and Hanken, J. (1996). Cranial neural-crest migration and chondrogenic fate in the Oriental fire-bellied toad *Bombina orientalis:* Defining the ancestral pattern of head development in anuran amphibians. *J. Morphol.* **229,** 105–120.

Roark, M., Sturtevant, M. A., Emery, J., Vaessin, H., Grell, E., and Bier, E. (1995). *Scratch,* a pan-neural gene encoding a zinc finger protein related to snail, promotes neuronal development. *Genes Dev.* **9,** 2384–2398.

Rubenstein, A., Merriam, J., and Klymkowsky, M. W. (1997). Localizing the adhesive and signaling functions of plakoglobin. *Dev. Genet.* **20,** 91–102.

Rupp, R. A. W., Snider, L., and Weintraub, H. (1994). *Xenopus* embryos regulate the nuclear localization of XMyoD. *Genes Dev.* **8,** 1311–1323.

Sadaghiani, B., and Thiebaud, C. H. (1987). Neural crest development in *Xenopus laevis* embryo, studied by interspecific transplantation and scanning electron microscopy. *Developmental Biology* **124,** 91–110.

Saint-Jeannet, J. P., He, X., Varmus, H. E., and Dawid, I. B. (1997). Regulation of dorsal fate in the neuraxis by Wnt-1 and Wnt-3a. *Proc. Natl. Acad. Sci. USA* **94,** 13713–13718.

Samakovlis, C., Manning, G., Steneberg, P., Hacohen, N., Cantera, R., and Krasnow, M. A. (1996). Genetic control of epithelial tube fusion during *Drosophila* tracheal development. *Development* **122,** 3531–3536

Sargent, M. G., and Bennett, M. F. (1990). Identification in *Xenopus* of a structural homologue of the *Drosophila* gene *Snail. Development* **109,** 967–973.

Savagner, P., Yamada, K. M., and Thiery, J. P. (1997). The zinc-finger protein *Slug* causes desmosome dissociation, an initial and necessary step for growth factor-induced epithelial–mesenchymal transition. *J. Cell Biol.* **137,** 1403–1419.

Sefton, M., Sanchez, S., and Nieto, M. A. (1998). Conserved and divergent roles for members of the *Snail* family of transcription factors in the chick and mouse embryo. *Development* **125,** 3111–3121.

Stoetzel, C., Bolcato-Bellemin, A. L., Bourgeois, P., Perrin-Schmitt, F., Meyer, D., Wolff, M., and Remy, P. (1998). *X-twi* is expressed prior to gastrulation in presumptive neuroectodermal and mesodermal cells in dorsalized and ventralized *Xenopus laevis* embryos. *Int. J. Dev. Biol.* **42,** 747–756.

Stone, L. W. (1926). Experiments showing the role of migrating neural crest (mesectoderm) in the formation of head skeleton and loose connective tissue in *Rana palustris. Roux's Arch. Entw. Mech.* **118,** 40–77.

Tanaka, M. M., Uemura, T., Oda, H., Takeichi, M., and Hayashi, S. (1996). Cadherin-mediated cell adhesion and cell motility in

Drosophila trachea regulated by the transcription factor Escargot. *Development* **122,** 3697–3705.

Thisse, C., Thisse, B., Schilling, T. F., and Postlethwait, J. H. (1993). Structure of the zebrafish *Snail*1 gene and its expression in wild-type, spadetail and no tail mutant embryos. *Development* **119,** 1203–1215.

Thisse, C., Thisse, B., and Postlethwait, J. H. (1995). Expression of *Snail2,* a second member of the zebrafish *Snail* family, in cephalic mesendoderm and presumptive neural crest of wild-type and spadetail mutant embryos. *Dev. Biol.* **172,** 86–99.

Trueb, L., and Hanken, J. (1992). Skeletal development in *Xenopus laevis* (Anura: Pipidae). *J. Morphol.* **214,** 1–41.

Whiteley, M., Noguchi, P. D., Sensabaugh, S. M., Odenwald, W. F., and Kassis, J. A. (1992). The *Drosophila* gene *Escargot* encodes a zinc finger motif found in *Snail*-related genes. *Mech. Dev.* **36,** 117–127.

Zernicka-Goetz, M., Pines, J., Ryan, K., Siemering, K. R., Haseloff, J., Evans, M. J., and Gurdon, J. B. (1996). An indelible lineage marker for *Xenopus* using a mutated green fluorescent protein. *Development* **122,** 3719–3724.

Received for publication January 4, 1999
Revised April 26, 1999
Accepted April 28, 1999